

# Impedance model for CdTe solar cells exhibiting constant phase element behaviour

G. Friesen<sup>a, b, \*</sup>, M.E. Özsar<sup>c</sup>, E.D. Dunlop<sup>a</sup>

<sup>a</sup>Joint Research Centre, Environment Institute, EC-DG JRC, ESTI, I-21020 Ispra (VA), Italy

<sup>b</sup>External PhD-student of the University of Konstanz, Konstanz, Germany

<sup>c</sup>BP Solar Technology Centre, 12 Brooklands Close, Windmill Rd., Sunbury-on-Thames, Middlesex TW16 7DX, UK

## Abstract

Different equivalent circuit models were used to fit the impedance spectra of CdTe solar cells at fixed d.c.-voltages and the resulting  $C$ - $V$  (capacitance–voltage)-curves and  $C$ - $f$  (capacitance–frequency)-curves were analysed. A simplified equivalent circuit model, which consists of a parallel resistor  $R_p$  and capacitor  $C$  in series with a resistor  $R_s$ , does not give a good fit to the experimental data and is not capable of simulating the dispersive trend. Also the commonly assumed model for CdTe, which consist of two sub-circuits ( $R_p$  and  $C$ ) does not allow the simulation of the measured impedance spectra. As both models are only consisting of frequency-independent circuit elements they can not be used to describe the frequency dispersion of thin film CdTe solar cells. A phenomenological description of the capacitance behaviour was obtained by replacing the capacitor of the first model by a frequency-dependent non-ideal capacitor, a so-called constant phase element (CPE). This element is described by the two CPE-parameters ( $T$  and  $P$ ). A correlation of these parameters to the capacitance dispersion and to the real cell capacitance are presented and the physical phenomena responsible for the capacitance dispersion are discussed. © 2000 Elsevier Science S.A. All rights reserved.

**Keywords:** CdTe; Impedance spectroscopy; Constant phase element; Capacitance dispersion

## 1. Introduction

Impedance spectroscopy (IS) [1] is the tool, generally employed by electrochemists to measure the kinetics of electrodes. However, this tool can be applied almost anywhere, and particularly to systems modelled by an equivalent circuit. From the equivalent circuit elements the physical parameters of a system can be calculated. This technique is particularly suitable if the circuit consists of one or two time constants, separated sufficiently or if one of them is dominant. In this study IS has been applied to measure the parameters of CdTe solar cells. The parameter measured or calculated by IS are the capacitance, the parallel resistance and the series resistance. The method used here is based on the frequency response analysis. The properties of a CdTe device can be defined in terms of its ability to store and transfer charge (i.e. its capacitance and conductance). IS records the response of a system to a small applied perturbation (i.e. a.c. signal), over a pre-determined frequency range. The applied ac voltage and the resultant ac current are measured and the impedance calculated

( $Z = V/I$ ). The technique is non-destructive and is particularly sensitive to small changes in the system. The resultant current has the same frequency  $\omega$  as the applied voltage but different phase  $\theta$  and amplitude  $|Z|$ . By measuring the complex impedance and separating the real and imaginary terms ( $Z'$  and  $Z''$ ) conductance  $G = 1/R$  and capacitance  $C$  may be calculated. From Eq. (1) the complex plane plot 'Nyquist plot' ( $Z'$  vs.  $Z''$ ), the capacitance dispersion  $C(\omega)$  and resistance dispersion  $R_p(\omega)$  are derived.

$$Z = V/I = V \sin \omega t / I \sin(\omega t + \theta) = Z' - iZ''$$

$$= (1/G) - i(1/\omega C) \quad (1)$$

The simplest equivalent circuit analysed in this study consists of a parallel resistor  $R_p$  and capacitor  $C$  in series with another resistor  $R_s$ . This model shown in Fig. 1a is used as starting point for the other two more complex models. If this simple cell model is valid the spectrum should be a semicircle, as shown in Fig. 1b. The characteristics of this semicircle are, the central point on the real axis  $Z'$ , a diameter of  $R_p$  displaced from the origin by  $R_s$ , the series resistance, and a maximum of  $Z''$  defined by Eq. (2).

$$Z''_{\max} = R_p = 1/\omega_{\max} C \quad (2)$$

\* Corresponding author. Tel.: +39-332-789-287; fax: +39-332-789-268.

E-mail address: gabi.friesen@jrc.it (G. Friesen)

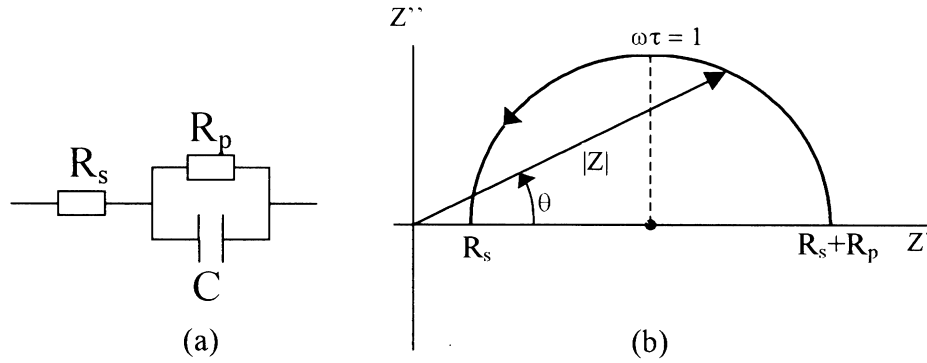


Fig. 1. RC-model (a) and resulting Nyquist plot (b).  $R_s$ , series resistance;  $R_p$ , parallel resistance;  $C$ , capacitance;  $Z'$ , real impedance;  $Z''$ , imaginary impedance;  $|Z|$ , absolute impedance;  $\theta$ , phase-shift;  $\omega$ , frequency;  $\tau$ , time-constant. The arrow indicate the direction of increasing frequency  $\omega$ .

The capacitance  $C$  is calculated from Eq. (2). The single RC-model leads to a semicircle that is characterised by a single time constant  $\tau$ , defined by Eq. (3).

$$\omega_{\max} = \tau^{-1} = (R_p C)^{-1} \quad (3)$$

It is known from literature [2] that the  $I$ - $V$  characteristic of CdTe solar cells can be simulated by a two-diode model. Typical behaviour such as roll over, cross over, fill factor loss and the trend of  $C$ - $V$  curves can be completely or partially explained by this model. The equivalent ac-circuit model is shown in Fig. 2a. It consists of two RC sub-circuits (parallel resistors:  $R_{p1}$ ,  $R_{p2}$  and capacitors:  $C_1$ ,  $C_2$ ) in series with a resistor  $R_s$ . It is assumed that the first of the two sub-circuits represents the junction and the second the back contact (Schottky contact). This double RC-model results in a two-time constant impedance spectrum as seen in Fig. 2b. How pronounced the two semicircles are depends on the ratio of the two time constants. If one of the two dominates only one semicircle will be visible. In the worst case the two-time constants lead to a distorted semicircle which make it difficult to separate the sub-circuits. Good starting values are needed for the fitting of the spectrum.

The CPE-model [1] shown in Fig. 3a is the third equivalent circuit model used in this study. It has the same structure as the single RC-model with the difference that the capacitor is replaced by a non-ideal frequency-dependent capacitor a so-called constant phase element (CPE).

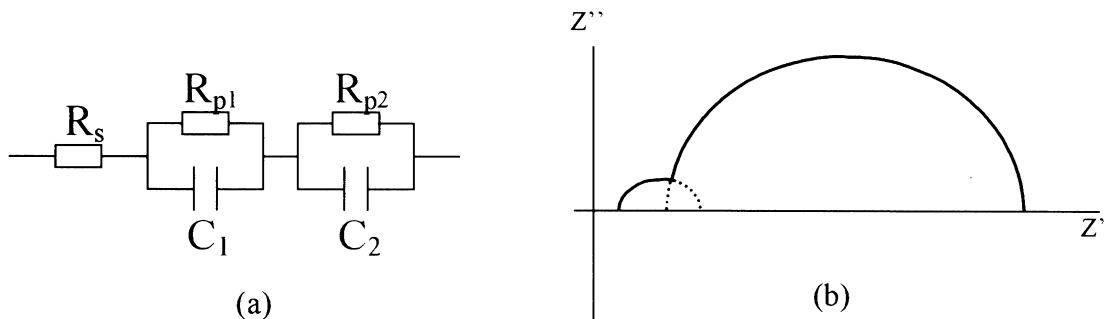


Fig. 2. Double RC-model (a) and resulting Nyquist plot (b).  $R_s$ , series resistance;  $R_{p1,2}$ , parallel resistances;  $C_{1,2}$ , capacitance's.

It is generally assumed that the non-ideal behaviour originates from a distribution in the current density due to material inhomogeneity. Fig. 3b shows the typical depressed semicircle obtained by such an equivalent circuit model. The depression originates from the fact that the distribution in the current density leads to a continuously or discretely distributed time constant  $\tau$ , which has a distribution around a mean value  $\tau_m = \omega_m^{-1}$ . This explains the displaced centre of the semicircle below the real axis. The angle  $\alpha$  (depression angle) by which such a semicircle is depressed below the real axis is related to the width of the time constant distribution. The impedance of a CPE, given by Eq. (4), is defined by the two values  $T$  and  $P$ , where  $T$  is a constant independent of frequency and  $P$  is a dimensionless parameter with a value between zero and unity. The real part of  $Z$  is resistive and is proportional to  $\omega^{-P}$ . The imaginary part is capacitive and is also proportional to  $\omega^{-P}$  (corresponding to a capacitance increasing with decreasing frequency according to  $\omega^{-(1-P)}$ ).

$$Z_{\text{CPE}} = 1/T(i\omega)^P \quad (4)$$

A distributed CPE-element has the characteristic that it can not be described by a finite number of discrete elements ( $R$ ,  $C$  and  $L$ ) with frequency independent values. However, for some values of  $P$  it simplifies to discrete elements: for  $P = 1$ , it is a capacitance and for  $P = 0$  a reciprocal of resistance. Usually for CdTe  $1 > P > 0.8$ , so it can be assumed that  $T$  has a more capacitive than resistive charac-

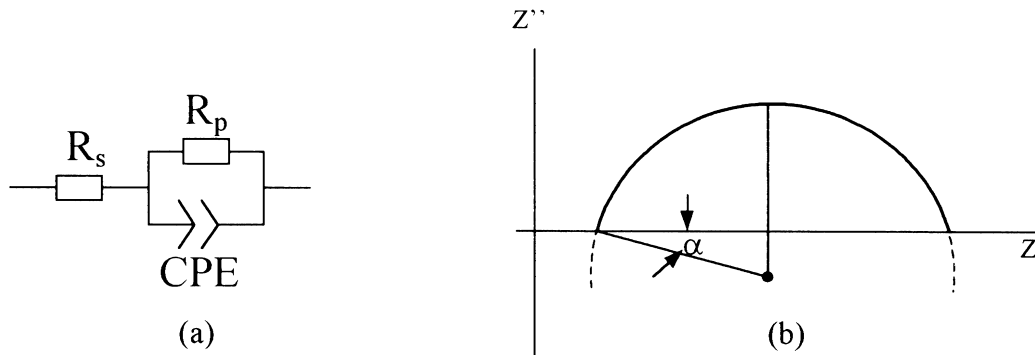


Fig. 3. CPE-model (a) and resulting Nyquist plot (b).  $R_s$ , series resistance;  $R_p$ , parallel resistance; CPE, constant phase element;  $\alpha$ , depression angle.

ter and that it is expressed in units of farads per square centimetre per second to the power  $P$ . The assumption that the cell capacitance  $C$  of a CdTe solar cell is equal to the parameter  $T$  is an error, or at least a crude simplification.  $T$  has to be interpreted as a non-ideal or pseudo-capacitance. The attempt to estimate the capacitance from CPE parameters ( $T$ ,  $P$ ) has been presented in a different publication. The relation derived by Sluyters and coworkers [3] for the calculation of the double-layer capacitance of an electrode has been used in this CdTe study. Eq. (5) shows the formula for the calculation of the cell capacitance.

$$T = C^P (R_s^{-1} + R_p^{-1})^{1-P} \quad (5)$$

As  $P$  gives information about the non-ideality of the cell capacitance it can be also related to the depression angle  $\alpha$  by Eq. (6).

$$\alpha = 90^\circ(1 - P) \quad (6)$$

An other way to determine the depression angle is to geometrically fit the depressed semicircle to a circle with a centre displaced from the real axis, but one has to be aware that a geometrical fit is not reliable as an equivalent circuit fit. It fits the displayed data to the equation for a circle and calculates values such as the diameter and location of the circle's centre. The frequency component is not used in these calculations.

## 2. Experimental

The test set-up consists of a Solartron 1260A frequency response analyser (FRA), of the device under test and a PC with the data acquisition and data evaluation software Z-plot [4]. The generator output of the FRA enables one to apply a small sinusoidal a.c.-signal superposed over a d.c.-voltage to the device. The ac-signal has to be less than the thermal voltage  $kT/q$ . This ensures a minimum deviation from the dc-conditions imposed. The relationship between the solar cell potential, measured by the differential voltage input of the FRA, and the current flow through the cell, measured by the current input of the FRA, allows one to determine the impedance of the device under test. Impedance spectra were

measured in the frequency range 1 MHz to 10 Hz with 10 steps per decade, distributed equally on a logarithmic scale to ensure evenly distributed measurement points. For all measurements a 10 mV a.c.-signal and d.c.-voltages between  $-1$  and  $0.8$  V were applied to the device under test. All measurements were executed under dark conditions and ambient temperature. The fitting and simulation of the acquired data were performed using the Z-plot software. The goodness of fit depends on the weighting type used for the analysis. It was found that the 'Calc-Modulus' weighting type, where each data points weight is normalised by its magnitude, gave the best fit results for CdTe IS-data. CdTe films (around  $2 \mu\text{m}$  thick) were electrodeposited on a thin ( $<1000 \text{ \AA}$ ) layer of chemical bath deposited (CBD) CdS on TO/glass substrates. Post-deposition annealing was carried out (without the use of  $\text{CdCl}_2$ ) at  $450^\circ\text{C}$ , 15 min, to type convert as-deposited CdTe from n to p to form n-CdS/p-CdTe devices. Small area ( $0.04 \text{ cm}^2$ ) cells were formed on CdTe using BP's proprietary back contact process.

## 3. Results and discussion

Some characteristic impedance spectra of a CdTe device (Nyquist plots) are shown in Fig. 4.

The spectra of Fig. 4a, measured at  $-1$ ,  $-0.5$ ,  $0$ ,  $0.1$ ,  $0.2$ , and  $0.44$  V are all characterised by a semicircular shape apparently composed by a single time constant (see Figs. 1 and 3). The size of these semicircles and the so resulting resistance and capacitance values show a clear voltage dependency. Starting from reverse bias the radius of the semicircle increases towards the maximum at zero bias and then decreases with increasing forward bias. For higher positive voltages ( $V > 0.5$  V) a distortion at the high frequency side of the semicircle (left end of the spectrum) starts to be visible. Fig. 4b shows an example measured at  $0.65$  V. This distortion could be due to a second RC-component added to the one of the junction. This additional component influences the shape of the spectrum at higher forward bias and leads to a two-time constant impedance spectrum as described in Fig. 2. As described in different

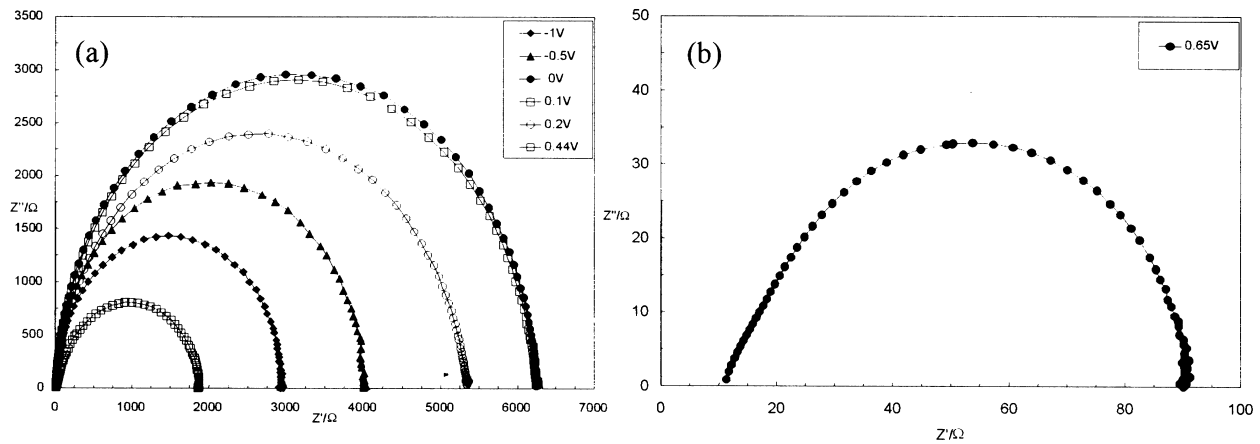


Fig. 4. Nyquist plot at different voltages for a CdTe sample under dark conditions and ambient temperature.

publications the second RC-element could be due to the back contact [2] or an interface, but as well other equivalent circuit models could be responsible for the tendency of the semicircle to flatten out at high frequencies. The attempt to separate the two RC sub-circuits did not lead to satisfactory results. A further investigation to find a model, which fits the experimental data for higher voltages, has to be found. From the investigations done until now we deduce that there is no double RC-model with frequency independent components, which can fit the experimental data. Because of this the modelling was limited to the simple RC- and CPE-model. Fig. 5 shows the impedance diagrams at three different voltages ( $-1$ ,  $0$  and  $0.2$  V) and their corresponding fits. First the semicircles were fitted by the simple RC-model, but no good fit could be achieved over the whole voltage range. The higher the applied voltage the higher the error. The deviation from the quasi-ideal semicircle shape to always more depressed semicircles and the observed capacitance dispersion (Fig. 6) justifies the use of the CPE-model. In the range of  $-1$  to  $0.8$  V very good fits of the impedance spectra were achieved.

The best way to see the good results obtained by the CPE-model is to look at a capacitance dispersion curve as shown

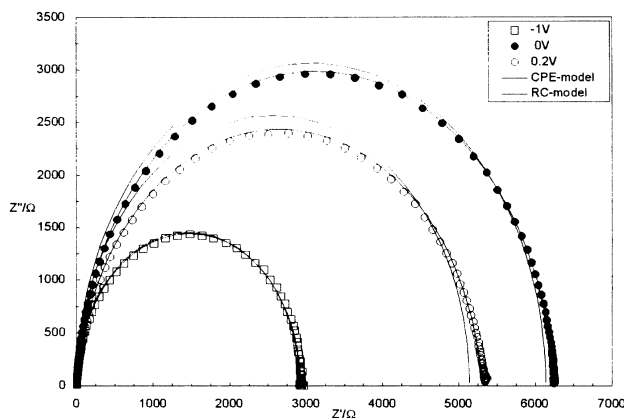


Fig. 5. Impedance spectra fitted by the RC- and CPE-model.

in Fig. 6a. It is demonstrated that contrary to the CPE-model the RC-model is not capable to fit the capacitance dispersion, which strongly influences all CdTe measurements. The published CdTe literature explains the frequency dispersion in terms of interface or bulk recombination in deep traps. The CPE-model enables a simulation of this frequency dependent trapping effect, which dominate all devices with high defect contents.

For reverse and forward bias ( $V < 0.45$  V) very good fits of the capacitance dispersion were achieved. For voltages higher than  $0.45$  V an increasing deviation in the low frequency range started to be visible (not shown in the graphs). Fig. 6b shows the voltage dependency of the capacitance dispersion. As described in the introduction the capacitance dispersion or non-ideal behaviour of the capacitance is correlated to the CPE-parameter  $P$ . The more  $P$  deviates from the ideal frequency independent capacitor assumed value  $P = 1$  the more the capacitance dispersion should be pronounced. Fig. 6b shows that in the range  $0$  to  $0.3$  V the capacitance dispersion increases with increasing forward bias and Fig. 7a shows as expected that  $P$  decreases. In the voltage range of  $-1$  to  $0.8$  V the  $P$ -value varies from  $0.99$  to  $0.85$  (Fig. 7a). For increasing negative voltages  $P$  tends to the ideal capacitor value  $P = 1$  but because of the inhomogeneity of the material and/or the grain-boundaries this ideal behaviour is never reached. In comparison homogenies devices such as monocrystalline silicon solar cells exhibit an impedance spectrum with a perfect semicircular shape and  $P = 1$ . As a CdTe device is forward biased the  $P$ -value decreases until a minimum value of approximately  $0.85$  is reached. The voltage dependence of the parameter  $P$  and so of the non-ideality and the frequency dispersion of the device is not fully resolved and has to be further investigated.

Additionally to the  $P$ -value extracted from the CPE-model Fig. 7a shows the depression angle  $\alpha_{\text{calc}}$  calculated by Eq. (6) and the angle  $\alpha_{\text{fit}}$  obtained by the geometric fit of the semi-circle. The trend of  $\alpha_{\text{fit}}$  and  $\alpha_{\text{calc}}$  are the same, but at positive voltages a deviation is visible. The errors

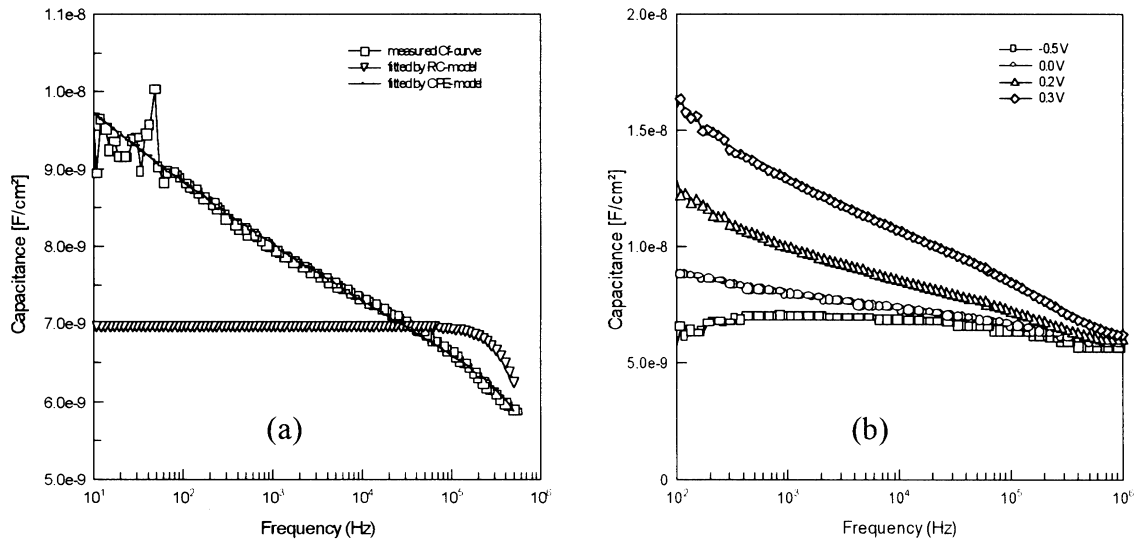


Fig. 6. (a) Capacitance dispersion fitted by the RC- and CPE-model and (b) capacitance dispersion at different voltages.

introduced by the simplified geometrical fit could be responsible for this deviation. Fig. 7b shows the pseudo-capacitance ( $T$ ) and capacitance-voltage curves obtained by impedance spectroscopy.  $T$  increases by two orders of magnitude and reaches a maximum between 0.5 and 0.6V. Compared to the positive voltage dependency the negative voltage dependency is moderate. To correlate the  $T$ -value to the cell capacitance Eq. (5) was used for the determination of the CV-curve. It is not clear if the applied formula is the best way to calculate the capacitance. It has to be noticed that because of the influence from the  $P$ -value the maximum visible in the pseudo-capacitance curve (CPE- $T$  in Fig. 7b) disappears after the transformation to the corresponding CV-curve. In dependence of the applied model (RC, CPE or geometrical) different CV-curves are plotted in Fig. 7b. As the RC-model gives

no satisfactory fit, especially at positive voltages, its CV-curve is plotted only for a limited voltage range.

#### 4. Conclusions

Usually the CPE is used for various systems showing strong frequency dispersion of the capacitance. It has been the subject of many papers about impedance spectroscopy of electrochemical systems but not of solar cells. In this paper the first results obtained by the use of this and other models are presented for CdTe solar cells.

Independent of the applied dc-voltage the simple RC-model does not fit the impedance spectra.

For higher forward bias ( $V > 0.5$  V) the impedance spectra are characterised by a second time constant or a distortion in the high frequency range.

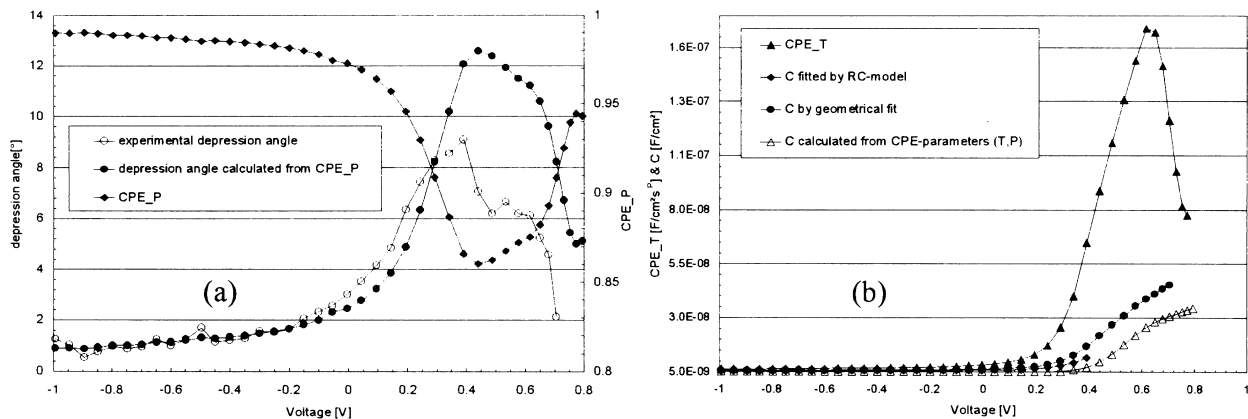


Fig. 7. (a) CPE-parameter  $P$  vs. voltage and comparison of the depression angle  $\alpha_{\text{calc}}$  calculated from Eq. (5) with the depression angle  $\alpha_{\text{fit}}$  obtained from a geometrical fit. (b) CPE- $P$  and different CV-curves obtained by fitting with the: (i) RC-model; (ii) CPE-model; and (iii) geometrical circle fit.

There is no double RC-model with frequency independent components which can fit the experimental data.

Only the CPE-model succeeded to fit the measured spectra over the whole voltage range.

In reverse bias  $P$  tends towards the ideal capacitance value  $P = 1$ , but because of the inhomogeneity of the material and/or the grain-boundaries this ideal behaviour is never reached.

The CPE-model allows to simulate the frequency dependent trapping effects of deep traps (interface and bulk) which are responsible for the in CdTe observed frequency dispersion.

The  $P$ -value varies from 0.99 to 0.85 and shows a minimum around 0.5 V.

The  $T$ -value is interpreted as a pseudo-capacitance and the real capacitance  $C$  has to be calculated from both CPE-parameters.

## Acknowledgements

The work presented here was partially supported by the European Commission, under the DGXII Non-Nuclear Energy Programme, contract number JOR3-CT97-0150.

## References

- [1] J.R. Mac Donald, W.B. Johnson, Impedance Spectroscopy, Wiley, New York, 1987.
- [2] A. Niemegeers, M. Burgelman, J. Appl. Phys. 81 (6) (1997) 2881.
- [3] G.J. Brug, A.L.G. Van Den Eeden, M. Sluyters-Rehbach, J.H. Sluyters, J. Electroanal. Chem. 176 (1984) 275.
- [4] Z-plot for Windows version 2.1: Electrochemical Impedance Software, Scribner Associates, Incorporated.